

# Experimental and numerical simulations of stone blocks at the archeological site of Volubilis, Morocco

Mohamed Sekkaki<sup>1</sup> and Khalil Naciri<sup>1</sup> and Ali Chaaba

<sup>1</sup> National Higher School of Engineering (ENSAM) Meknes, Morocco

**Abstract.** This study aims to compare the results obtained experimentally on a stone sample used in the construction of the Triumphal Arch of Caracalla in the archaeological site of Volubilis with those obtained numerically by two implemented models: the Concrete Model (CM) implemented in ANSYS software and the Concrete Damage Plasticity (CDP) model implemented in ABAQUS software. The objective is to determine the suitable model for accurately simulating the stones used in Roman heritage structures. Compression and tensile tests were carried out on cylindrical stone specimens. A comparison of the mechanical behavior of the stone was made between the experimental results and those from the two numerical models.

**Keywords:** Volubilis, simulation, experimental, masonry.

## 1 Introduction

The archaeological site of Volubilis in Morocco (**Fig 1**) dates back to the Roman Empire. The site comprises historic monuments, the majority of which are masonry structures. Over the years, these structures have suffered several types of damage, including cracks in their stone blocks (**Fig 2**). This makes these historic monuments unstable.

To preserve and strengthen these structures, it is essential to assess their structural behavior with regard to external stresses. To achieve this, laboratory tests are required to evaluate mechanical properties and determine failure modes under various loads. These tests are complemented by numerical simulations using models implemented in simulation software such as ANSYS and ABAQUS. The Concrete Model (CM) and Concrete Damage Plasticity (CDP) model are used to simulate quasi-fragile materials such as stone, which have non-linear strength characteristics. Several studies have been conducted to simulate masonry structures using both CM and CDP [1], [2], [3], [4], [5], [6], [7]. However, while these models are typically used for concrete structures, their

application to natural materials, such as the stones used in Roman architecture remains a relatively unexplored research topic. This gap raises the question of the accuracy of the modeling software used in predicting the mechanical behavior of natural stones, particularly in the context of their conservation.

Our study aims to compare the experimental and numerical results of a uniaxial compression test carried out on the stones used in the construction of the Triumphal Arch of Caracalla in the archaeological site of Volubilis, Morocco. Numerical simulations were carried out using CM and CDP models implemented in the ANSYS and ABAQUS software, respectively. The results focus on the stress-strain response, zones of weakness, and failure modes. This comparison enabled the identification of the most suitable numerical model that yields results closest to the experimental data and to make recommendations regarding the appropriate modeling approach for studying stone behavior at the Volubilis site.

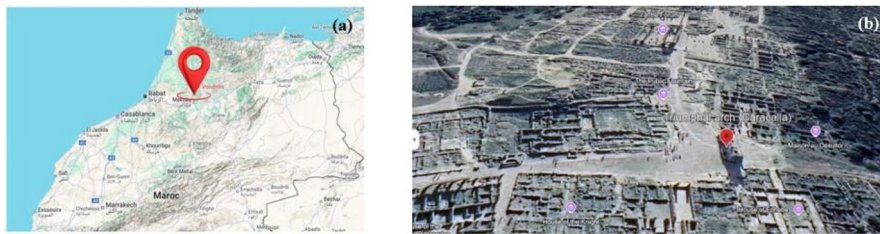


**Fig 1.** Volubilis site: (a) Geographical location; (b) General view



**Fig 2.** Cracks in the Stone Blocks of the Triumphal Arch in Volubilis

## 2 Experimental characterization of stone

To perform the experimental tests on the stone samples, a preparation process was followed. Firstly, stone samples were collected from the original quarry, called “Moulay Driss”. They were cored in an arbitrary direction using a core drill and then cut into cylindrical specimens with dimensions of 50mmx50mm. Next, two experimental tests were conducted using a PROETI-type mechanical press: the compressive strength test and the tensile strength test.

The compression test was performed by applying axial displacement progressively and uniformly to three specimens until failure, in accordance with the ASTM C39 standard [8]. **Table 1** summarizes the mechanical property values for each sample tested. The results indicate an average compressive strength of 81.83 MPa, which reflects the high strength of the stone. The material exhibits a modulus of elasticity approaching 109 GPa, indicating a very rigid material. These values confirm that the stone used to build the Triumphal Arch has superior mechanical properties, which enhance the durability of the structure over time.

Fracture mode analysis revealed predominantly longitudinal cracking characterized by vertical cracks and splitting, as shown in **Fig 5.a**. The stress-strain curves obtained during the compression test (**Fig 7**) show a gradual stress rise until the elastic limit, followed by abrupt failure with no significant plastic deformation.

The indirect tensile test was carried out on three specimens in accordance with ASTM D3967 standard [9]. The tensile strength of the material as found to be 7.5 MPa, which is approximately 8% of the compressive strength. These experimental results are used to validate the numerical simulations conducted in this study.

**Table 1.** Mechanical properties of stone samples

Sample	Mechanical properties		
	Compressive strength (MPa)	Tensile strength (MPa)	Young's modulus (GPa)
1	81.50	7	108.5
2	82.10	8,2	110.2
3	81.90	7,4	108.9

### 3 Numerical simulation

#### 3.1 Concrete Model

The "Concrete" model implemented in ANSYS commercial software predicts the failure of brittle materials (in three spatial directions). This model is based on Williams-Warnke yield criterion developed by K.J. Wiliam and E.P. Warnke in the 1970s.

This model requires the definition of five parameters :

- Compressive strength  $f_c$ ;
- Tensile strength  $f_t$ ;
- Biaxial compressive strength  $f_{cb}$ ;
- Open shear transfer coefficient  $\beta_o$ ;

Compressive and tensile strength,  $f_c$  and  $f_t$  respectively, are determined through laboratory testing. In contrast, biaxial compressive strength is calculated using the following formula [10]:

$$f_{cb} = 1.2f_c \tag{1}$$

The two shear transfer coefficients,  $\beta_o$  and  $\beta_c$ , correspond to open and closed crack conditions, respectively; and are used to simulate shear slip along the crack face.

According to Razaghi et al. [11], the coefficient  $\beta_o$  typically ranges between 0.2 and 0.5, while the  $\beta_c$  ranges between 0.0 (indicating total loss of shear transfer) and 1.0 (indicating no shear transfer loss).

**Fig 3.** illustrates the failure surface proposed by William-Warnke. These surfaces are represented in an orthogonal coordinate system  $(O, \sigma_{xp}, \sigma_{yp})$ .

The input parameters for this model are shown in **Table 2**.

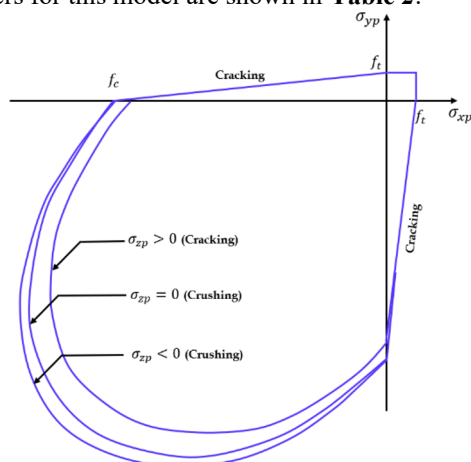


**Fig 3.** Failure surface suggested by Wiliam and Warnke (Based on [10])

**Table 2.** Mechanical properties and input parameters of stones

Parameter	Value
Young's modulus $E$ (MPa)	109000
Poisson's coefficient $\nu$	0,25
Uniaxial compressive strength $f_c$ (MPa)	81.83
Uniaxial tensile strength $f_t$ (MPa)	7,5
Density (Kg/m3)	2960
Biaxial compressive strength $f_{cb}$ (MPa)	98,2
Open shear transfer coefficient $\beta_o$	0,2
Closed shear transfer coefficient $\beta_c$	0,2

### 3.2 Concrete Damage Plasticity

The concrete damaged plasticity model is a plasticity-damage-based model introduced by [12] and further developed by [13] to predict the behavior of concrete, rock, and other quasi-brittle materials. The two main failure modes of this model are cracking in tension and crushing in compression.

CDP is defined by means of the following parameters: dilation angle  $\psi$ , eccentricity  $\epsilon$ , the ratio  $\sigma_{b0}/\sigma_{c0}$  between biaxial compressive yield strength and uniaxial compressive

yield strength. The parameter  $K_c$ , hardening-softening compressive behavior, tensile softening behavior. Further details of these parameters' meaning found in [14].

The parameters  $K_c$ ,  $\sigma_{b0}/\sigma_{c0}$ , and  $\epsilon$  were assumed as suggested in the ABAQUS manual [14] for quasi-brittle materials. The dilation angle was taken equal to  $10^\circ$ , as it is commonly used in the literature. The inelastic compressive behavior was extracted from the experimental test derived on the stone. The tensile behavior was estimated according to [15], [16] based on the stone experimental tensile strength. Hence, the adopted input parameters are summarized in **Table 3**, **Table 4** and **Table 5**.

**Table 3.** Abaqus input mechanical characteristics

Reference	[14]			Estimated	Experimental	[17]	Experimental	Experimental
Parameter	$K_c$	$\sigma_{b0}/\sigma_{c0}$	$\epsilon$	$\Psi$	Elastic modulus (MPa)	Poisson's ratio	Compressive strength (MPa)	Tensile strength (MPa)
Value	0.67	1.16	0.1	$10^\circ$	109000	0.25	81.83	7.5

**Table 4.** Inelastic compressive behavior

Inelastic strain	Yield stress (MPa)
0	81.83
3.25714E-05	80.02
5.25714E-05	74.89
0.000122571	54.04
0.000272571	35.91
0.000332571	30.45

**Table 5.** Inelastic tensile behavior

Cracking displacement (mm)	Yield stress (MPa)
0	7.5
0.001	7.16950169
0.003	6.55155495
0.005	5.98686967
0.01	4.77901446
0.02	3.04519722
0.03	1.94040554
0.04	1.23643015
0.05	0.78785567
0.06	0.50202315
0.07	0.31989012
0.08	0.2038346

## 4 Results and discussion of the numerical simulation

This section presents an analysis of the results obtained from the numerical simulations in comparison with the experimental test. The aim is to compare the values obtained through laboratory testing with those obtained from modelling, to assess the accuracy of the approaches adopted. **Fig 4.** illustrates the simulated stone geometry.

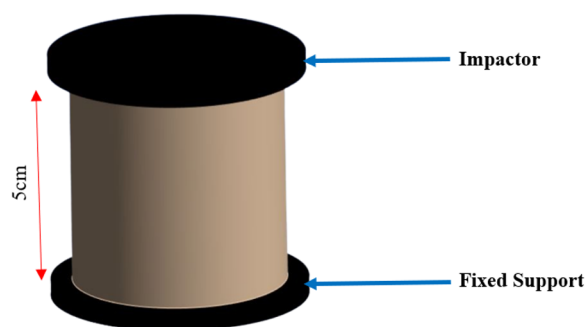


**Fig 4.** Geometry of simulated stone

### 4.1 Concrete Model results

This section presents the results obtained numerically using ANSYS software via the concrete model. Figure 5.b shows the stress distribution in the simulated stone. The failure is marked in red, located on the sides of the cylindrical specimen, which corresponds to the cracking mechanisms observed during the experimental tests. Figure 5.c shows the cracking and crushing points of the material, with a high concentration of cracks in the upper and lower areas of the specimen. The red points indicate large cracks, while the green points indicate internal microcracks.

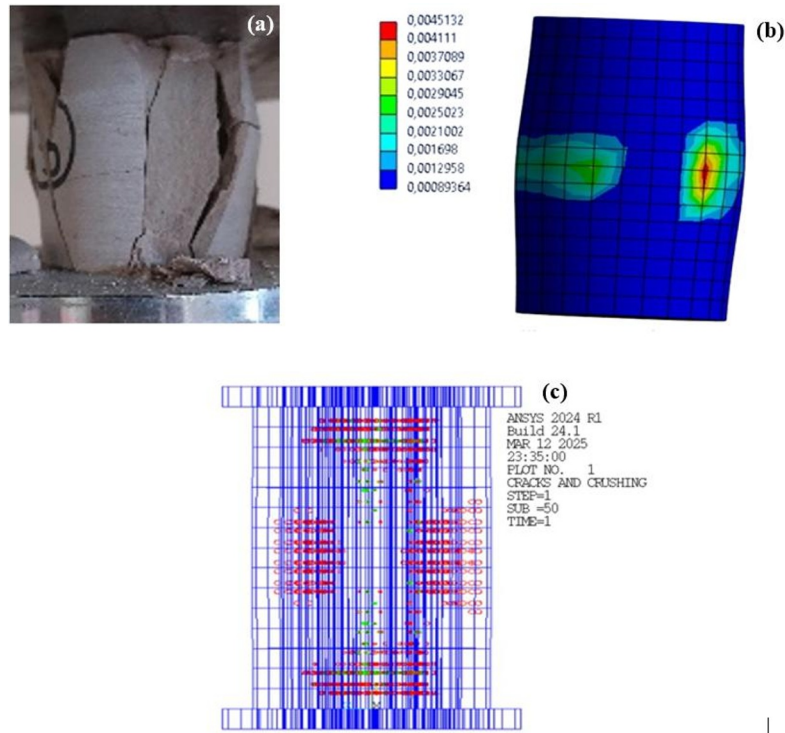


**Fig 5.** Failure modes comparison: (a) experimental failure mode (b) numerical failure mode (c) crack and crushing distribution

#### 4.2 CDP model results

To illustrate the crack location and failure modes obtained by the CDP model, the variables PEEQ and PEEQT are introduced. These are scalar measures computed from plastic strain components. A value greater than 0 for PEEQ and PEEQT indicates cracks formation in compression (compressive crushing) and tension (tensile cracking) respectively. At the point of failure, horizontal cracks were located in the middle of the specimen due to crushing in compression, combined with vertical cracks due to tension forces.

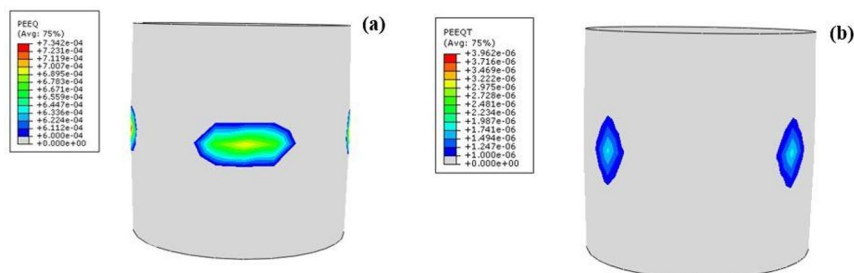


**Fig 6.** Distribution of (a) PEEQ; and (b) PEEQT

### 4.3 Comparison between the two models

Based on the numerical results obtained by both the Concrete Model and CDP, as well as the experimental test results on stone samples, it was found that the Concrete Model provides more accurate results for simulating the behavior of stone under compression. The compressive strength obtained by the Concrete model is about 82.20 MPa. Consequently, the value obtained is very close to that obtained experimentally (81.83 MPa). However, the compressive strength obtained by CDP is about 79.61 MPa, which indicates an underestimation of the compressive strength compared to experimental tests. **Erreur ! Source du renvoi introuvable.** shows the stress-strain curves obtained for the two models in comparison with those obtained experimentally. The ANSYS Concrete Model simulated the elastic phase followed by failure at a stress of 82.20 MPa. This agrees with experimental results. Furthermore, the deformation observed after fracture in the numerical simulations showed a similar behavior to that observed in experimental testing, which the CDP model did not capture. Thus, the Concrete Model in ANSYS is better for simulating the stone of the Triumphal Arch. The concrete model also showed a stress distribution very close to that observed in experimental tests. In contrast, the CDP model shows a more localized stress distribution, which does not reflect reality. In conclusion, the CDP model provides satisfactory results, while the ANSYS concrete model offers more accurate results to simulate the mechanical behavior of the stones of the Volubilis site

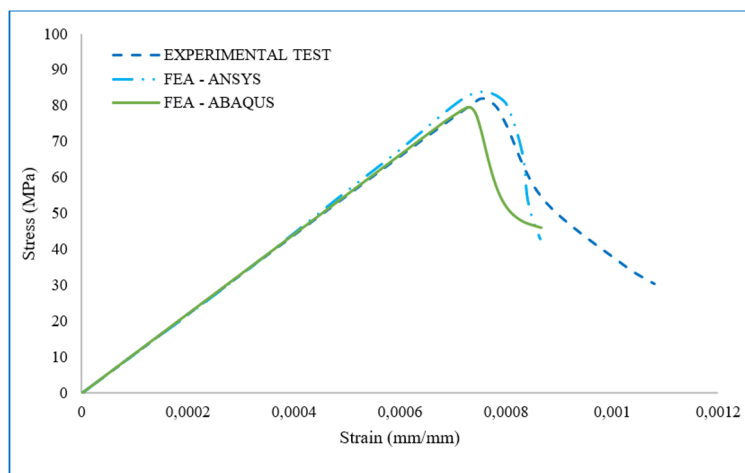


Fig 7. Experimental and numerical stress-strain curves

## 5 Conclusion

In this work, a comparative study was carried out between experimental results and those obtained numerically on a stone sample from the Triumphal Arch at the archaeological site of Volubilis. Two experimental tests were conducted in the laboratory, namely the uniaxial compressive strength test and the split tensile test. Both tests showed that the stone has a high compressive strength of 81.83 MPa and a tensile

strength of 7.5 MPa. The failure mode was characterized by vertical cracks and splintering. These results were complemented by two numerical simulations using two modeling approaches: the Concrete Model and Concrete Damage Plasticity (CDP) model, implemented respectively in ANSYS and ABAQUS. The results obtained from these two models demonstrated different levels of accuracy. The failure mode obtained using the Concrete Model was very close to that observed experimentally, while the compressive strength predicted by the CDP model showed an underestimation of the experimental value.

In this respect, the results obtained clearly show that the Concrete Model implemented in ANSYS software provides a better understanding of the mechanical behavior of the existing stones at the Volubilis archaeological site

**Disclosure of Interests.** The authors have no competing interests to declare that are relevant to the content of this article.

## References

1. M. Sekkaki, A. Chaaba, and I. Aalil, "Numerical simulation of a dry joint masonry arch in the Volubilis site (Morocco)," *Materials Today: Proceedings*, Jul. 2023, doi: 10.1016/j.matpr.2023.07.022.
2. J. I. Gisbert, D. Bru, A. Gonzalez, and S. Ivorra, "Masonry micromodels using high order 3D elements," *Procedia Structural Integrity*, vol. 11, pp. 428–435, Jan. 2018, doi: 10.1016/j.prostr.2018.11.055.
3. M. Sekkaki and A. Chaaba, "Failure Analysis of Masonry Walls in 2D and 3D Subjected to Combined Compression and Shear Loading", doi: 10.13189/cea.2024.120614.
4. K. Naciri, I. Aalil, and A. Chaaba, "Masonry compressive behavior simulation using detailed micro-modeling approach," in 2020 1st International Conference on Innovative Research in Applied Science, Engineering and Technology (IRASET), Apr. 2020, pp. 1–5. doi: 10.1109/IRASET48871.2020.9092275.
5. K. Naciri, I. Aalil, A. Chaaba, and M. Al-Mukhtar, "Numerical modeling of a masonry arch structure," *Procedia Structural Integrity*, vol. 37, pp. 469–476, Jan. 2022, doi: 10.1016/j.prostr.2022.01.111.
6. K. Naciri, I. Aalil, A. Chaaba, and M. Al-Mukhtar, "Detailed Micromodeling and Multiscale Modeling of Masonry under Confined Shear and Compressive Loading," *Pract. Period. Struct. Des. Constr.*, vol. 26, no. 1, p. 04020056, Feb. 2021, doi: 10.1061/(ASCE)SC.1943-5576.0000538.
7. K. Naciri, I. Aalil, A. Chaaba, and M. Al-Mukhtar, "Numerical analysis of the brick shape and bond pattern effects on the masonry cyclic behavior: a new brick shape to improve the masonry seismic performance," *Asian J Civ Eng*, vol. 23, no. 1, pp. 67–86, Jan. 2022, doi: 10.1007/s42107-021-00409-5.
8. "Standard Test Method for Compressive Strength of Cylindrical Concrete Specimens." Accessed: Mar. 26, 2025. [Online]. Available: [https://store.astm.org/c0039\\_c0039m-21.html](https://store.astm.org/c0039_c0039m-21.html)
9. "Standard Test Method for Splitting Tensile Strength of Cylindrical Concrete Specimens." Accessed: Mar. 26, 2025. [Online]. Available: <https://store.astm.org/c0496-96.html>
10. S. Ahmad, B. M. Irons, and O. C. Zienkiewicz, "Theory Reference for the Mechanical APDL and Mechanical Applications," 2009.

11. J. Razaghi, A. Hosseini, and F. Hatami, "Finite element method application in nonlinear analysis of reinforced concrete structures." Accessed: Jan. 29, 2024. [Online]. Available: <https://scholar.googleusercontent.com/scholar.bib?q=info:gK-G96LjDJoJ:scholar.google.com/&output=citation&scisdr=CIHZ9cIuEN-POlxDd3cE:AFWwaeYAAAAAZbfbxcGR2fmV2rBg9-q5VCLZ52o&scisig=AFWwaeYAAAAAZbfbxZADChz-A0lA256qxp17fiw&scisf=4&ct=citation&cd=-1&hl=fr>
12. J. Lubliner, J. Oliver, S. Oller, and E. Oñate, "A plastic-damage model for concrete," *International Journal of Solids and Structures*, vol. 25, no. 3, pp. 299–326, Jan. 1989, doi: 10.1016/0020-7683(89)90050-4.
13. J. Lee and G. L. Fenves, "Plastic-Damage Model for Cyclic Loading of Concrete Structures," Aug. 1998, Accessed: Mar. 29, 2025. [Online]. Available: <https://ascelibrary.org/doi/10.1061/%28ASCE%290733-9399%281998%29124%3A8%28892%29>
14. ABAQUS, ABAQUS analysis user's manual, 6.10 ed. Dassault Systèmes Simulia Corp., 2010.
15. A. J. Aref and K. M. Dolatshahi, "A three-dimensional cyclic meso-scale numerical procedure for simulation of unreinforced masonry structures," *Computers and Structures*, vol. 120, pp. 9–23, 2013, doi: 10.1016/j.compstruc.2013.01.012.
16. A. Drougkas, P. Roca, and C. Molins, "Numerical prediction of the behavior, strength and elasticity of masonry in compression," *Engineering Structures*, vol. 90, pp. 15–28, 2015, doi: 10.1016/j.engstruct.2015.02.011.
17. H. Gercek, "Poisson's ratio values for rocks," *International Journal of Rock Mechanics and Mining Sciences*, vol. 44, no. 1, pp. 1–13, Jan. 2007, doi: 10.1016/j.ijrmms.2006.04.011.